# Comparative Assessment Of The Role Of CT Versus MIRI In Diagnosis Of Biliary Obstruction

An ESSAY
Submitted For Partial Fulfillment Of Master Degree In Radiodiagnosis

#### **Presented By**

**Mohammed Ali Mohammed Assar** M.B., B.Ch.

#### **Supervised By**

#### Dr. Maha Hussein Anwar AbdelSalam

Assistant Professor of Radiodiagnosis Faculty Of Medicine Ain Shams University

#### **Dr** . Mohammed Shaker Ghazy

Lecturer of Radiodiagnosis Faculty Of Medicine Ain Shams University

> Radiodiagnosis Department Faculty of Medicine Ain Shams University 2010

# بسم الله الرحمن الرحيم



صدق الله العظيم (سورة الرحمن: الآية 1 و 2)

## <u>Acknowledgment</u>

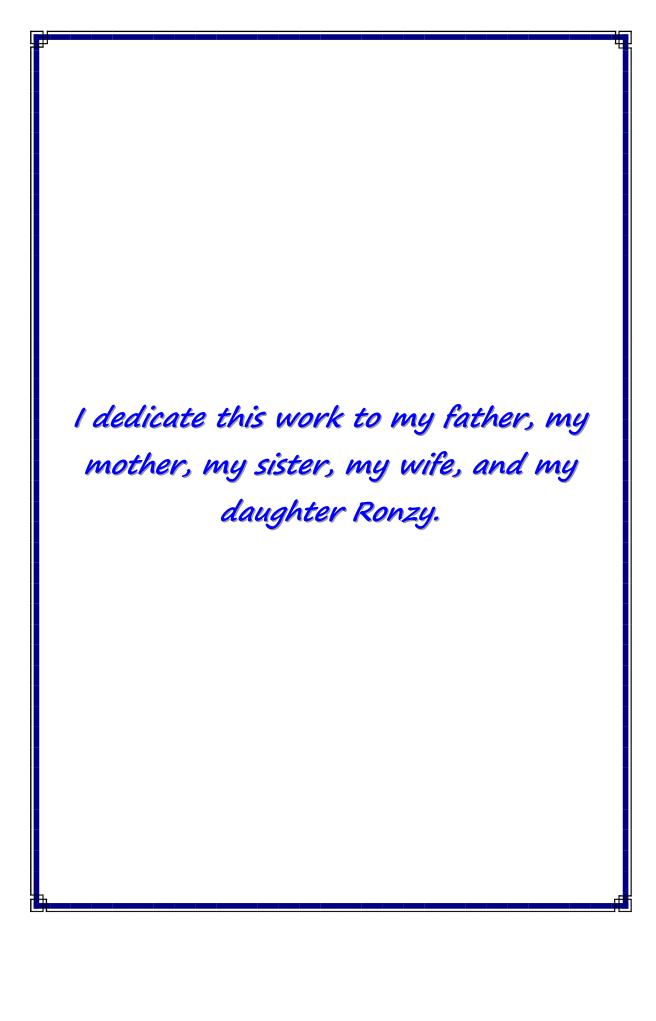
## First of all thanks to Allah

I would like to present my sincere thanks and appreciation to **Prof. Dr. Maha Hussein Anwar**, Assistant Professor of Radiodiagnosis, Faculty of Medicine, Ain Shams University, who guided this work and helped whenever I was in need. Her great patience, close supervision, and constant encouragement throughout this work are beyond my words of thanks.

I would like to express my deepest gratitude and appreciation to **Dr. Mohammed Shaker Ghazy**, Lecturer of Radiodiagnosis, Faculty of Medicine, Ain Shams University, for his meticulous supervision, remarkable guidance and great backing.

Finally, I would like to express my deepest gratitude for the constant support, understanding and love that I received from my family and my friends during this work.

Mohammed Ali Assar May, 2010



# **CONTENTS**

List Of Figures	II
List Of Tables	VII
List Of Abbreviations	VIII
Chapter I. Introduction and Aim of the work	1
Chapter II. Anatomy of the biliary system	5
Chapter III	15
CT anatomy of the biliary system	
MRI anatomy of the biliary system	
Chapter IV. Pathology of biliary obstruction	43
Chapter V	57
CT techniques of examination of the biliary tree	
MRI techniques of examination of the biliary tree	76
Chapter VI. CT & MRI findings in biliary obstruction	109
Chapter VII. Summary And Conclusion	147
Chapter VIII. References	150
Chapter IX. Arabic summary	168

## **List of Figures**

No.	Title	Page		
1	Overall arrangement of the intrahepatic and extrahepatic biliary tree	6		
2	Drawing illustrates the hepatic segmental anatomy as			
	described by Couinaud.			
3	Intrahepatic ductand biliary confluence anatomy.	8		
4	Interior of the gallbladder and bile ducts.	10		
5	Drawing illustrates the normal biliary tract.	12		
6	The bile duct and pancreatic duct merge to form the hepato-	13		
	pancreatic ampulla.			
7	Diagram of pancreatic ductal anatomic variants.	14		
8	Normal CTcholangiogram MIP	16		
9	Normal intrahepatic ducts by contrast-enhanced computed	17		
	tomography.			
10	Normal anatomy of extrahepatic bile duct on CT	19		
11	CT scan shows normal common hepatic duct at level of porta	20		
	hepatis.	21		
12	12 Contrast-enhanced computed tomography demonstrates a			
	fluid-attenuation gallbladder.	22		
13	13 Contrast-enhanced CT scan reveals normal appearance of			
	gallbladder in coronal plane.			
14	Anatomic variations of GB on CT	24		
15	Axial CT scan shows the normal cystic duct	25		
16	(A) Drawings illustrate howthe cystic duct may insert into the	26		
	extrahepatic bile duct. (B) Axial CT scan shows parallel			
	cystic duct.	25		
17	CT scan shows normal common bile duct	27		
18	CT scan of a normal pancreatic duct.	29		
19	Normal MRCP findings.	30		
20	Normal hepatic ductal anatomy on projective MR	31		
	cholangiogram.	32		
21	21 (A) Projective coronal MR cholangiogram shows tributaries			
	of common hepatic duct. (B) Projective M R cholangiogram			
22	shows drainage of right posterior duct into left hepatic duct.  (A) Projective MP, shelppingsom shave reversel of normal	22		
22	(A) Projective MR cholangiogram shows reversal of normal	33		
	relationship of right posterior duct and right anterior duct. (B)			
	Projective MR cholangiogram shows triple confluence of			
	right anterior duct, right posterior duct, and left hepatic duct.			

23 (A) Projective image showing the gallbladder, common hepatic duct, and right (R) and left (L) hepatic ducts. (B)T2-weighted image demonstrating the pancreatic duct, the common bile duct, the common hepatic duct, and the duodenum.  24 Magnetic resonance cholangiopancreatography of normal gallbladder, common duct, and pancreatic duct on oblique thick-slab image.  25 A)T1-and (B)T2-weighted images showing GB sludge. (C) and (D) showing GB septum.  26 Coronal oblique MR cholangiopancreatogram demonstrates the normal cystic duct  27 (A) Projective MR cholangiogram shows medial and low insertion of the cystic duct. (B) Projective MR cholangiogram shows parallel course of cystic duct and common hepatic duct. (C) Projective MR cholangiogram shows long cystic duct (D) Projective MR cholangiogram shows long cystic duct remnant.  28 Maximum intensity projection MRCP image shows normal common duct, main pancreatic duct, and gallbladder.  29 Normal pancreatic duct on MR multiplanar reformatted image.  30 (A) MR cholangiopancreatogram reveals a vertically oriented pancreatic duct. (B) MR pancreatogram demonstrates a loop in the pancreatic duct.  31 Magnetic resonance cholangiopancreatography shows the dominant dorsal pancreatic duct.  32 shows the two types of gallstones.  33 A diagram shows pancreatic head cancer obstructs the CBD.  48 Schematic diagram for sites of cholangiocarcinoma.  51 Classification of cancers of the human biliary tract.  52 36 CT oblique coronal reformation.  63 37 CT curved planar reformation.  64 38 CT minimum intensity projection.  65 39 Sequential axial CT cholangiogram images.  70 MDCT IV cholangiogram.  71 41 MDCT Direct Cholangiogram.  72 42 Susceptibility artifacts on MRI.			
common bile duct, the common hepatic duct, and the duodenum.  24 Magnetic resonance cholangiopancreatography of normal gallbladder, common duct, and pancreatic duct on oblique thick-slab image.  25 A)Tl-and (B)T2-weighted images showing GB sludge. (C) and (D) showing GB septum.  26 Coronal oblique MR cholangiopancreatogram demonstrates the normal cystic duct  27 (A) Projective MR cholangiogram shows medial and low insertion of the cystic duct. (B) Projective MR cholangiogram shows parallel course of cystic duct and common hepatic duct. (C) Projective MR cholangiogram shows high insertion of cystic duct remnant.  28 Maximum intensity projection MRCP image shows normal common duct, main pancreatic duct, and gallbladder.  29 Normal pancreatic duct on MR multiplanar reformatted image.  30 (A) MR cholangiopancreatogram reveals a vertically oriented pancreatic duct. (B) MR pancreatogram demonstrates a loop in the pancreatic duct.  31 Magnetic resonance cholangiopancreatography shows the dominant dorsal pancreatic duct.  32 shows the two types of gallstones.  33 A diagram shows pancreatic head cancer obstructs the CBD.  34 Schematic diagram for sites of cholangiocarcinoma.  35 Classification of cancers of the human biliary tract.  36 CT oblique coronal reformation.  37 CT curved planar reformation.  38 CT minimum intensity projection.  39 Sequential axial CT cholangiogram images.  70  40 MDCT IV cholangiogram.  71	23	hepatic duct, and right (R) and left (L) hepatic ducts. (B)T2-	
duodenum.  24 Magnetic resonance cholangiopancreatography of normal gallbladder, common duct, and pancreatic duct on oblique thick-slab image.  25 A)T1-and (B)T2-weighted images showing GB sludge. (C) and (D) showing GB septum.  26 Coronal oblique MR cholangiopancreatogram demonstrates the normal cystic duct  27 (A) Projective MR cholangiogram shows medial and low insertion of the cystic duct. (B) Projective MR cholangiogram shows parallel course of cystic duct and common hepatic duct. (C) Projective MR cholangiogram shows high insertion of cystic duct remnant.  28 Maximum intensity projection MRCP image shows normal common duct, main pancreatic duct, and gallbladder.  29 Normal pancreatic duct on MR multiplanar reformatted image.  30 (A) MR cholangiopancreatogram reveals a vertically oriented pancreatic duct. (B) MR pancreatogram demonstrates a loop in the pancreatic duct.  31 Magnetic resonance cholangiopancreatography shows the dominant dorsal pancreatic duct.  32 shows the two types of gallstones.  33 A diagram shows pancreatic head cancer obstructs the CBD.  34 Schematic diagram for sites of cholangiocarcinoma.  51 Classification of cancers of the human biliary tract.  52 CT curved planar reformation.  63 CT oblique coronal reformation.  64 38 CT minimum intensity projection.  65 Sequential axial CT cholangiogram images.  70 MDCT IV cholangiogram.  71 MDCT Direct Cholangiogram.			
Magnetic resonance cholangiopancreatography of normal gallbladder, common duct, and pancreatic duct on oblique thick-slab image.  25 A)T1-and (B)T2-weighted images showing GB sludge. (C) and (D) showing GB septum.  26 Coronal oblique MR cholangiopancreatogram demonstrates the normal cystic duct  27 (A) Projective MR cholangiogram shows medial and low insertion of the cystic duct. (B) Projective MR cholangiogram shows parallel course of cystic duct and common hepatic duct. (C) Projective MR cholangiogram shows high insertion of cystic duct. (D) Projective MR cholangiogram shows long cystic duct remnant.  28 Maximum intensity projection MRCP image shows normal common duct, main pancreatic duct, and gallbladder.  29 Normal pancreatic duct on MR multiplanar reformatted image.  30 (A) MR cholangiopancreatogram reveals a vertically oriented pancreatic duct. (B) MR pancreatogram demonstrates a loop in the pancreatic duct.  31 Magnetic resonance cholangiopancreatography shows the dominant dorsal pancreatic duct.  32 shows the two types of gallstones.  33 A diagram shows pancreatic head cancer obstructs the CBD.  34 Schematic diagram for sites of cholangiocarcinoma.  35 Classification of cancers of the human biliary tract.  36 CT oblique coronal reformation.  37 CT curved planar reformation.  38 CT minimum intensity projection.  39 Sequential axial CT cholangiogram images.  70 MDCT IV cholangiogram.  71 MDCT Direct Cholangiogram.			
gallbladder, common duct, and pancreatic duct on oblique thick-slab image.  25 A)T1-and (B)T2-weighted images showing GB sludge. (C) and (D) showing GB septum.  26 Coronal oblique MR cholangiopancreatogram demonstrates the normal cystic duct  27 (A) Projective MR cholangiogram shows medial and low insertion of the cystic duct. (B) Projective MR cholangiogram shows parallel course of cystic duct and common hepatic duct. (C) Projective MR cholangiogram shows high insertion of cystic duct. (D) Projective MR cholangiogram shows long cystic duct remnant.  28 Maximum intensity projection MRCP image shows normal common duct, main pancreatic duct, and gallbladder.  29 Normal pancreatic duct on MR multiplanar reformatted image.  30 (A) MR cholangiopancreatogram reveals a vertically oriented pancreatic duct. (B) MR pancreatogram demonstrates a loop in the pancreatic duct.  31 Magnetic resonance cholangiopancreatography shows the dominant dorsal pancreatic duct.  32 shows the two types of gallstones.  34 Schematic diagram for sites of cholangiocarcinoma.  35 Classification of cancers of the human biliary tract.  36 CT oblique coronal reformation.  37 CT curved planar reformation.  38 CT minimum intensity projection.  39 Sequential axial CT cholangiogram images.  70 MDCT IV cholangiogram.  71	24		2.5
thick-slab image.  25 A)T1-and (B)T2-weighted images showing GB sludge. (C) and (D) showing GB septum.  26 Coronal oblique MR cholangiopancreatogram demonstrates the normal cystic duct  27 (A) Projective MR cholangiogram shows medial and low insertion of the cystic duct. (B) Projective MR cholangiogram shows parallel course of cystic duct and common hepatic duct. (C) Projective MR cholangiogram shows high insertion of cystic duct. (D) Projective MR cholangiogram shows long cystic duct remnant.  28 Maximum intensity projection MRCP image shows normal common duct, main pancreatic duct, and gallbladder.  29 Normal pancreatic duct on MR multiplanar reformatted image.  30 (A) MR cholangiopancreatogram reveals a vertically oriented pancreatic duct. (B) MR pancreatogram demonstrates a loop in the pancreatic duct.  31 Magnetic resonance cholangiopancreatography shows the dominant dorsal pancreatic duct.  32 shows the two types of gallstones.  33 A diagram shows pancreatic head cancer obstructs the CBD.  34 Schematic diagram for sites of cholangiocarcinoma.  35 Classification of cancers of the human biliary tract.  36 CT oblique coronal reformation.  37 CT curved planar reformation.  38 CT minimum intensity projection.  39 Sequential axial CT cholangiogram images.  70 MDCT IV cholangiogram.  71 MDCT Direct Cholangiogram.	24		35
25 A)T1-and (B)T2-weighted images showing GB sludge. (C) and (D) showing GB septum.  26 Coronal oblique MR cholangiopancreatogram demonstrates the normal cystic duct  27 (A) Projective MR cholangiogram shows medial and low insertion of the cystic duct. (B) Projective MR cholangiogram shows parallel course of cystic duct and common hepatic duct. (C) Projective MR cholangiogram shows high insertion of cystic duct. (D) Projective MR cholangiogram shows long cystic duct remnant.  28 Maximum intensity projection MRCP image shows normal common duct, main pancreatic duct, and gallbladder.  29 Normal pancreatic duct on MR multiplanar reformatted image.  30 (A) MR cholangiopancreatogram reveals a vertically oriented pancreatic duct. (B) MR pancreatogram demonstrates a loop in the pancreatic duct.  31 Magnetic resonance cholangiopancreatography shows the dominant dorsal pancreatic duct.  32 shows the two types of gallstones.  33 A diagram shows pancreatic head cancer obstructs the CBD.  34 Schematic diagram for sites of cholangiocarcinoma.  35 Classification of cancers of the human biliary tract.  36 CT oblique coronal reformation.  37 CT curved planar reformation.  38 CT minimum intensity projection.  39 Sequential axial CT cholangiogram images.  70 MDCT IV cholangiogram.  71 MDCT Direct Cholangiogram.			
and (D) showing GB septum.  26 Coronal oblique MR cholangiopancreatogram demonstrates the normal cystic duct  27 (A) Projective MR cholangiogram shows medial and low insertion of the cystic duct. (B) Projective MR cholangiogram shows parallel course of cystic duct and common hepatic duct. (C) Projective MR cholangiogram shows high insertion of cystic duct remnant.  28 Maximum intensity projection MRCP image shows normal common duct, main pancreatic duct, and gallbladder.  29 Normal pancreatic duct on MR multiplanar reformatted image.  30 (A) MR cholangiopancreatogram reveals a vertically oriented pancreatic duct. (B) MR pancreatogram demonstrates a loop in the pancreatic duct.  31 Magnetic resonance cholangiopancreatography shows the dominant dorsal pancreatic duct.  32 shows the two types of gallstones.  33 A diagram shows pancreatic head cancer obstructs the CBD.  34 Schematic diagram for sites of cholangiocarcinoma.  35 Classification of cancers of the human biliary tract.  36 CT oblique coronal reformation.  37 CT curved planar reformation.  38 CT minimum intensity projection.  39 Sequential axial CT cholangiogram images.  70 MDCT IV cholangiogram.  71 MDCT Direct Cholangiogram.	25		26
26 Coronal oblique MR cholangiopancreatogram demonstrates the normal cystic duct  27 (A) Projective MR cholangiogram shows medial and low insertion of the cystic duct. (B) Projective MR cholangiogram shows parallel course of cystic duct and common hepatic duct. (C) Projective MR cholangiogram shows high insertion of cystic duct. (D) Projective MR cholangiogram shows long cystic duct remnant.  28 Maximum intensity projection MRCP image shows normal common duct, main pancreatic duct, and gallbladder.  29 Normal pancreatic duct on MR multiplanar reformatted image.  30 (A) MR cholangiopancreatogram reveals a vertically oriented pancreatic duct. (B) MR pancreatogram demonstrates a loop in the pancreatic duct.  31 Magnetic resonance cholangiopancreatography shows the dominant dorsal pancreatic duct.  32 shows the two types of gallstones.  43 A diagram shows pancreatic head cancer obstructs the CBD.  48 Schematic diagram for sites of cholangiocarcinoma.  51 Classification of cancers of the human biliary tract.  52 36 CT oblique coronal reformation.  63 CT curved planar reformation.  64 CT minimum intensity projection.  65 Sequential axial CT cholangiogram images.  70 MDCT IV cholangiogram.  71 MDCT Direct Cholangiogram.	23		30
the normal cystic duct  27 (A) Projective MR cholangiogram shows medial and low insertion of the cystic duct. (B) Projective MR cholangiogram shows parallel course of cystic duct and common hepatic duct. (C) Projective MR cholangiogram shows high insertion of cystic duct. (D) Projective MR cholangiogram shows long cystic duct remnant.  28 Maximum intensity projection MRCP image shows normal common duct, main pancreatic duct, and gallbladder.  29 Normal pancreatic duct on MR multiplanar reformatted image.  30 (A) MR cholangiopancreatogram reveals a vertically oriented pancreatic duct. (B) MR pancreatogram demonstrates a loop in the pancreatic duct.  31 Magnetic resonance cholangiopancreatography shows the dominant dorsal pancreatic duct.  32 shows the two types of gallstones.  43 A diagram shows pancreatic head cancer obstructs the CBD.  48 Schematic diagram for sites of cholangiocarcinoma.  51 Classification of cancers of the human biliary tract.  52 Schematic diagram for sites of cholangiocarcinoma.  53 CT oblique coronal reformation.  64 CT oblique coronal reformation.  65 Sequential axial CT cholangiogram images.  70 MDCT IV cholangiogram.  71 MDCT Direct Cholangiogram.	26		37
27 (A) Projective MR cholangiogram shows medial and low insertion of the cystic duct. (B) Projective MR cholangiogram shows parallel course of cystic duct and common hepatic duct. (C) Projective MR cholangiogram shows high insertion of cystic duct. (D) Projective MR cholangiogram shows long cystic duct remnant.  28 Maximum intensity projection MRCP image shows normal common duct, main pancreatic duct, and gallbladder.  29 Normal pancreatic duct on MR multiplanar reformatted image.  30 (A) MR cholangiopancreatogram reveals a vertically oriented pancreatic duct. (B) MR pancreatogram demonstrates a loop in the pancreatic duct.  31 Magnetic resonance cholangiopancreatography shows the dominant dorsal pancreatic duct.  32 shows the two types of gallstones.  47 A diagram shows pancreatic head cancer obstructs the CBD.  34 Schematic diagram for sites of cholangiocarcinoma.  35 Classification of cancers of the human biliary tract.  36 CT oblique coronal reformation.  37 CT curved planar reformation.  38 CT minimum intensity projection.  39 Sequential axial CT cholangiogram images.  70 MDCT IV cholangiogram.  71 MDCT Direct Cholangiogram.	20		31
insertion of the cystic duct. (B) Projective MR cholangiogram shows parallel course of cystic duct and common hepatic duct. (C) Projective MR cholangiogram shows high insertion of cystic duct. (D) Projective MR cholangiogram shows long cystic duct remnant.  28 Maximum intensity projection MRCP image shows normal common duct, main pancreatic duct, and gallbladder.  29 Normal pancreatic duct on MR multiplanar reformatted image.  30 (A) MR cholangiopancreatogram reveals a vertically oriented pancreatic duct. (B) MR pancreatogram demonstrates a loop in the pancreatic duct.  31 Magnetic resonance cholangiopancreatography shows the dominant dorsal pancreatic duct.  32 shows the two types of gallstones.  47 A diagram shows pancreatic head cancer obstructs the CBD.  48 Schematic diagram for sites of cholangiocarcinoma.  51 Classification of cancers of the human biliary tract.  52 A CT oblique coronal reformation.  63 CT curved planar reformation.  64 CT minimum intensity projection.  65 Sequential axial CT cholangiogram images.  70 MDCT IV cholangiogram.  71 MDCT Direct Cholangiogram.	27	•	38
cholangiogram shows parallel course of cystic duct and common hepatic duct. (C) Projective MR cholangiogram shows high insertion of cystic duct. (D) Projective MR cholangiogram shows long cystic duct remnant.  28 Maximum intensity projection MRCP image shows normal common duct, main pancreatic duct, and gallbladder.  29 Normal pancreatic duct on MR multiplanar reformatted image.  30 (A) MR cholangiopancreatogram reveals a vertically oriented pancreatic duct. (B) MR pancreatogram demonstrates a loop in the pancreatic duct.  31 Magnetic resonance cholangiopancreatography shows the dominant dorsal pancreatic duct.  32 shows the two types of gallstones.  47 33 A diagram shows pancreatic head cancer obstructs the CBD.  48 34 Schematic diagram for sites of cholangiocarcinoma.  51 35 Classification of cancers of the human biliary tract.  52 36 CT oblique coronal reformation.  63 37 CT curved planar reformation.  64 38 CT minimum intensity projection.  65 39 Sequential axial CT cholangiogram images.  70 MDCT IV cholangiogram.  71 MDCT Direct Cholangiogram.	21		30
common hepatic duct. (C) Projective MR cholangiogram shows high insertion of cystic duct. (D) Projective MR cholangiogram shows long cystic duct remnant.  28 Maximum intensity projection MRCP image shows normal common duct, main pancreatic duct, and gallbladder.  29 Normal pancreatic duct on MR multiplanar reformatted image.  30 (A) MR cholangiopancreatogram reveals a vertically oriented pancreatic duct. (B) MR pancreatogram demonstrates a loop in the pancreatic duct.  31 Magnetic resonance cholangiopancreatography shows the dominant dorsal pancreatic duct.  32 shows the two types of gallstones.  47 33 A diagram shows pancreatic head cancer obstructs the CBD.  48 34 Schematic diagram for sites of cholangiocarcinoma.  51 35 Classification of cancers of the human biliary tract.  52 36 CT oblique coronal reformation.  63 37 CT curved planar reformation.  64 38 CT minimum intensity projection.  65 39 Sequential axial CT cholangiogram images.  70 MDCT IV cholangiogram.  71 MDCT Direct Cholangiogram.		3	
shows high insertion of cystic duct. (D) Projective MR cholangiogram shows long cystic duct remnant.  28 Maximum intensity projection MRCP image shows normal common duct, main pancreatic duct, and gallbladder.  29 Normal pancreatic duct on MR multiplanar reformatted image.  30 (A) MR cholangiopancreatogram reveals a vertically oriented pancreatic duct. (B) MR pancreatogram demonstrates a loop in the pancreatic duct.  31 Magnetic resonance cholangiopancreatography shows the dominant dorsal pancreatic duct.  32 shows the two types of gallstones.  47 A diagram shows pancreatic head cancer obstructs the CBD.  48 Schematic diagram for sites of cholangiocarcinoma.  51 Classification of cancers of the human biliary tract.  52 Cr oblique coronal reformation.  63 CT oblique coronal reformation.  64 CT minimum intensity projection.  65 Sequential axial CT cholangiogram images.  70 MDCT IV cholangiogram.  71 MDCT Direct Cholangiogram.			
cholangiogram shows long cystic duct remnant.  28 Maximum intensity projection MRCP image shows normal common duct, main pancreatic duct, and gallbladder.  29 Normal pancreatic duct on MR multiplanar reformatted image.  30 (A) MR cholangiopancreatogram reveals a vertically oriented pancreatic duct. (B) MR pancreatogram demonstrates a loop in the pancreatic duct.  31 Magnetic resonance cholangiopancreatography shows the dominant dorsal pancreatic duct.  32 shows the two types of gallstones.  47 As Schematic diagram for sites of cholangiocarcinoma.  51 Classification of cancers of the human biliary tract.  52 CT oblique coronal reformation.  63 CT curved planar reformation.  64 CT minimum intensity projection.  65 Sequential axial CT cholangiogram images.  70 MDCT IV cholangiogram.  71 MDCT Direct Cholangiogram.			
28 Maximum intensity projection MRCP image shows normal common duct, main pancreatic duct, and gallbladder.  29 Normal pancreatic duct on MR multiplanar reformatted image.  30 (A) MR cholangiopancreatogram reveals a vertically oriented pancreatic duct. (B) MR pancreatogram demonstrates a loop in the pancreatic duct.  31 Magnetic resonance cholangiopancreatography shows the dominant dorsal pancreatic duct.  32 shows the two types of gallstones.  33 A diagram shows pancreatic head cancer obstructs the CBD.  34 Schematic diagram for sites of cholangiocarcinoma.  35 Classification of cancers of the human biliary tract.  36 CT oblique coronal reformation.  37 CT curved planar reformation.  38 CT minimum intensity projection.  39 Sequential axial CT cholangiogram images.  40 MDCT IV cholangiogram.  71 MDCT Direct Cholangiogram.			
common duct, main pancreatic duct, and gallbladder.  29 Normal pancreatic duct on MR multiplanar reformatted image.  30 (A) MR cholangiopancreatogram reveals a vertically oriented pancreatic duct. (B) MR pancreatogram demonstrates a loop in the pancreatic duct.  31 Magnetic resonance cholangiopancreatography shows the dominant dorsal pancreatic duct.  32 shows the two types of gallstones.  33 A diagram shows pancreatic head cancer obstructs the CBD.  34 Schematic diagram for sites of cholangiocarcinoma.  35 Classification of cancers of the human biliary tract.  36 CT oblique coronal reformation.  37 CT curved planar reformation.  38 CT minimum intensity projection.  39 Sequential axial CT cholangiogram images.  40 MDCT IV cholangiogram.  71 MDCT Direct Cholangiogram.	28		39
image.  30 (A) MR cholangiopancreatogram reveals a vertically oriented pancreatic duct. (B) MR pancreatogram demonstrates a loop in the pancreatic duct.  31 Magnetic resonance cholangiopancreatography shows the dominant dorsal pancreatic duct.  32 shows the two types of gallstones.  33 A diagram shows pancreatic head cancer obstructs the CBD.  34 Schematic diagram for sites of cholangiocarcinoma.  35 Classification of cancers of the human biliary tract.  36 CT oblique coronal reformation.  37 CT curved planar reformation.  38 CT minimum intensity projection.  39 Sequential axial CT cholangiogram images.  40 MDCT IV cholangiogram.  71 MDCT Direct Cholangiogram.  74			
30 (A) MR cholangiopancreatogram reveals a vertically oriented pancreatic duct. (B) MR pancreatogram demonstrates a loop in the pancreatic duct.  31 Magnetic resonance cholangiopancreatography shows the dominant dorsal pancreatic duct.  32 shows the two types of gallstones.  33 A diagram shows pancreatic head cancer obstructs the CBD.  34 Schematic diagram for sites of cholangiocarcinoma.  35 Classification of cancers of the human biliary tract.  36 CT oblique coronal reformation.  37 CT curved planar reformation.  38 CT minimum intensity projection.  39 Sequential axial CT cholangiogram images.  40 MDCT IV cholangiogram.  71 MDCT Direct Cholangiogram.	29	Normal pancreatic duct on MR multiplanar reformatted	40
pancreatic duct. (B) MR pancreatogram demonstrates a loop in the pancreatic duct.  31 Magnetic resonance cholangiopancreatography shows the dominant dorsal pancreatic duct.  32 shows the two types of gallstones.  33 A diagram shows pancreatic head cancer obstructs the CBD.  34 Schematic diagram for sites of cholangiocarcinoma.  35 Classification of cancers of the human biliary tract.  36 CT oblique coronal reformation.  37 CT curved planar reformation.  38 CT minimum intensity projection.  39 Sequential axial CT cholangiogram images.  40 MDCT IV cholangiogram.  41 MDCT Direct Cholangiogram.  74		•	
in the pancreatic duct.  Magnetic resonance cholangiopancreatography shows the dominant dorsal pancreatic duct.  Shows the two types of gallstones.  A diagram shows pancreatic head cancer obstructs the CBD.  Schematic diagram for sites of cholangiocarcinoma.  Classification of cancers of the human biliary tract.  CT oblique coronal reformation.  CT curved planar reformation.  CT minimum intensity projection.  Sequential axial CT cholangiogram images.  MDCT IV cholangiogram.  MDCT Direct Cholangiogram.  MDCT Direct Cholangiogram.	30		41
31Magnetic resonance cholangiopancreatography shows the dominant dorsal pancreatic duct.4232shows the two types of gallstones.4733A diagram shows pancreatic head cancer obstructs the CBD.4834Schematic diagram for sites of cholangiocarcinoma.5135Classification of cancers of the human biliary tract.5236CT oblique coronal reformation.6337CT curved planar reformation.6438CT minimum intensity projection.6539Sequential axial CT cholangiogram images.7040MDCT IV cholangiogram.7141MDCT Direct Cholangiogram.74			
dominant dorsal pancreatic duct.  32 shows the two types of gallstones.  47  33 A diagram shows pancreatic head cancer obstructs the CBD.  48  34 Schematic diagram for sites of cholangiocarcinoma.  51  35 Classification of cancers of the human biliary tract.  52  36 CT oblique coronal reformation.  63  37 CT curved planar reformation.  64  38 CT minimum intensity projection.  59 Sequential axial CT cholangiogram images.  40 MDCT IV cholangiogram.  71  41 MDCT Direct Cholangiogram.  74		1	
32shows the two types of gallstones.4733A diagram shows pancreatic head cancer obstructs the CBD.4834Schematic diagram for sites of cholangiocarcinoma.5135Classification of cancers of the human biliary tract.5236CT oblique coronal reformation.6337CT curved planar reformation.6438CT minimum intensity projection.6539Sequential axial CT cholangiogram images.7040MDCT IV cholangiogram.7141MDCT Direct Cholangiogram.74	31		42
33A diagram shows pancreatic head cancer obstructs the CBD.4834Schematic diagram for sites of cholangiocarcinoma.5135Classification of cancers of the human biliary tract.5236CT oblique coronal reformation.6337CT curved planar reformation.6438CT minimum intensity projection.6539Sequential axial CT cholangiogram images.7040MDCT IV cholangiogram.7141MDCT Direct Cholangiogram.74		•	
34Schematic diagram for sites of cholangiocarcinoma.5135Classification of cancers of the human biliary tract.5236CT oblique coronal reformation.6337CT curved planar reformation.6438CT minimum intensity projection.6539Sequential axial CT cholangiogram images.7040MDCT IV cholangiogram.7141MDCT Direct Cholangiogram.74			
35Classification of cancers of the human biliary tract.5236CT oblique coronal reformation.6337CT curved planar reformation.6438CT minimum intensity projection.6539Sequential axial CT cholangiogram images.7040MDCT IV cholangiogram.7141MDCT Direct Cholangiogram.74		<u> </u>	
36CT oblique coronal reformation.6337CT curved planar reformation.6438CT minimum intensity projection.6539Sequential axial CT cholangiogram images.7040MDCT IV cholangiogram.7141MDCT Direct Cholangiogram.74			
37CT curved planar reformation.6438CT minimum intensity projection.6539Sequential axial CT cholangiogram images.7040MDCT IV cholangiogram.7141MDCT Direct Cholangiogram.74		J	
38CT minimum intensity projection.6539Sequential axial CT cholangiogram images.7040MDCT IV cholangiogram.7141MDCT Direct Cholangiogram.74			
39Sequential axial CT cholangiogram images.7040MDCT IV cholangiogram.7141MDCT Direct Cholangiogram.74		<u> </u>	
40MDCT IV cholangiogram.7141MDCT Direct Cholangiogram.74			
41 MDCT Direct Cholangiogram. 74			
42 Susceptibility artifacts on MRI. 79			
± ✓	42	Susceptibility artifacts on MRI.	79

43	(A) Coronal 2D SSFSE thin-section image, (B) corresponding coronal 3D FRFSE image, (C) Oblique	81
	coronal 2D SSFSE thick-slab image, (D) oblique coronal MIP reconstruction from the 3D FRFSE data.	
4.4		92
44	Anterior thick-section half-Fourier rapid acquisition with relaxation enhancement MR cholangiopancreatogram.	82
45	Breath-hold HASTE MR cholangiopancreatography.	83
46	(A) Source MRCP image shows filling defects within the	87
	gallbladder. (B) MIP reconstructed image does not depict the	
	filling defects.	
47	(A) MIP reconstructed image from a study performed during	87
	an incomplete breath hold demonstrates a respiratory motion	
	artifact mimicking a duplicated main pancreatic duct, (B)	
	MIP reconstructed image from a repeat study reveals a	
	normal appearing main pancreatic duct.	
48	(A) Single-slice MRCP image shows aerobilia, (B) Axial T2-	88
	weighted image shows aerobilia.	
49	(A) Multi-section MRCP image shows false stenosis of the	89
	common hepatic duct, (B) Drip-infusion cholangiogram	
	reveals three surgical clips near the normal common hepatic	
	duct.	
50	MRCP image shows prominent duodenal papilla.	89
51	Pseudo-obstruction of the dilated common hepatic duct due	90
	to compression by the right hepatic artery on MRI.	
52 Axial T2 weighted MR image reveals the close a		103
	relation between the common bile duct and the gastro	
	duodenal artery.	
53	In Phase Gradient Echo Axial Breath Hold.	103
54	Different view projections: (A) RAO, (B) LAO, (C) Axial.	106
55	Thick slab MRCP.	106
56	(A) Coronal and (B) sagittal MinIP CT images demonstrate	111
	two large CBD stones, (C) CT cholangiography using axial	
	oblique thin slab MinIP depicts multiple intrahepatic bile	
	duct stones.	
57	(A) Appearance of stone., (B) A distal CBD stone presenting	112,
	as rim sign, (C) A stone in distal portion of CBD, (D) a stone	113
	completely surrounded by bile (target sign), (E) Stone in	
	CBD seen in hypoattenuating bile on CECT scan, (F)	
	Calcified stone in CBD seen on CECT scan.	

58	Choledocolithiasis. (A)Thick- slab T2-weighted magnetic resonance cholangiopancreatography, (B) Thin slice T2-	115
50	weighted magnetic resonance imaging	117
59	Multislice CT with curved coronal reformat displaying a	117
	pancreatic head tumour obstructing the common bile duct and	
	pancreatic duct.	
60	Non-resectable pancreatic adenocarcinoma with arterial encasement.	117
61	Coronal oblique MR cholangiopancreatogram demonstrates	119
	pancreatic duct obstruction.	
62	Depiction of pancreatic head adenocarcinoma on MRCP.	120
63	Unrespectable pancreatic carcinoma on MRI.	121
64	T1-weighted images obtained (A), (B) before and (C), (D)	122
	after intravenous administration of manganese-DPDP.	
65	T2 weighted axial MRI shows pancreatic carcinoma.	123
66	CT scan obtained during the (A) HAP and (B) PVP shows	125
	Periductal Infiltrating CC.	
67	Intrahepatic cholangiocarcinoma (A) Noncontrast (CT), (B)	126
	Portal venous phase CT, (C) after 10-minute delay.	
68	Intrahepatic intraductal cholangiocarcinoma. (A) Contrast-	127
	enhanced computed tomography, (B) Delayed image.	
69	Extrahepatic cholangiocarcinoma on Contrast-enhanced CT.	128
70	Hilar cholangiocarcinoma (Klatskin tumor). (A) Coronal MR	129
	cholangiogram obtained with a single-section half-Fourier	
	RARE sequence, (B) Axial fat-suppressed T2-weighted fast	
	spin-echo MR image, (C) Axial T1-weighted gradient-echo	
	MR image obtained after injection of gadolinium cm	
71	Intra-hepatic cholangiocarcinoma. (A) Axial arterial phase	131
	contrast-enhanced 3D GRE T1WI, (B) On an axial delayed	
	phase contrast-enhanced 3D GRE T1WI.	
72	Gallbladder carcinoma presentations on CT.	132
73	Gallbladder carcinoma. (A) CT scan shows mass in	134
	gallbladder fossa. (B) Associated biliary obstruction.	
74	Metastasis to the gallbladder. (A) Non-contrast CT, (B)	135
	Contrast-enhanced CT, (C) Portal phase image.	
75	Adenomyomatosis of the gallbladder on CT.	136
76	MRCP revealed the presence of a gallbladder tumor.	137
77	Axial fat-suppressed T2-weighted MR image shows	138
	carcinoma arising in a porcelaneous gallbladder.	

78	CT showing a double duct dilatation sign.	139
79	Coronal MR cholangiogram shows severe dilatation of the	
	biliary tree and obstruction at the level of the ampulla.	
80	Ampullary carcinoma of the nodular mass type. (A) 14	
	Schematic drawing, (B) Single-section MRCP image,	142
	Coronal (C) and axial (D)T2-weighted SSFSE images.	
81	CT shows (A) periductal LNs, (B) multiple liver metastases.	143
82	Coronal MIP of 3D-SSFP shows metastatic disease to the	
	pancreatic head.	
83	PSC. (A) CT scan shows finding of pruning. (B) CT scan	145
	shows isolated, dilated penipheral ducts.	
84	PSC. (A) Contrast-enhanced T1-weighted image, (B)Thick-	146
	slab magnetic resonance cholangiopancreatography.	

## **List of Tables**

No.	Title		
1	Scanning parameters for abdominal imaging for three different	62	
	MDCT scanners.		
2	MRCP Pulse Sequences.	76	
3	Locator SSFSE imaging parameters.	101	
4	Axial T2 imaging parameters.	102	
5	Axial in-phase (fat saturation) imaging parameters.	104	
6	MRCP (Thin Slice) imaging parameters.	105	
7	MRCP (Thick Slice) imaging parameters.	107	
8	Common causes of biliary obstruction.	110	

#### **List of Abbreviations**

2D-FSE	Two dimensional fast spin echo
3D-FSE	Three dimensional fast spin echo
CBD	Common Bile Duct
CC	Cholangiocarcinoma
CDL	Choledocholitiasis
CE	Contrast enhanced
CE-FAST	Contrast enhanced fourier acquired steady state sequence
CHD	Common hepatic duct
CPR	Curved planar reformation
CT	Computed Tomography
CTC	Computed Tomography Cholangiography
EHBDS	Extrahepatic bile ducts
ENBD	Endoscopic naso-biliary drainage
ERCP	Endoscopic Retrograde Cholangiopancreatography
ERBD	Endoscopic retrograde biliary drainage
FRFSE	Fast-Recovery Fast Spin-Echo
FSE	Fast Spin Echo
GB	Gallbladder
GMN	Gradient Moment Nulling
GRE	Gradient Echo Imaging
HAP	Hepatic arterial phase
HASTE	Half-Fourier Single-shot Turbo spin Echo
HU	Hounsfield Unit
IHBDS	Intrahepatic bile ducts
IR	Inversion recovery
IV	Intravenous
LAO	Left Anterior Oblique
MDCT	Multi-detector Computed tomography
MinIP	Minimum Intensity Projection
MIP	Maximum Intensity Projection
Mn-DPDP	Manganese-dipyridoxyl diphosphate
MPR	Muliplanar reformation
MRCP	Magnetic Resonance Cholangiopancreatography
MRI	Magnetic Resonance Imaging
PACS	Picture Archiving And Communication Systems

PD	Pancreatic duct
PSC	Primary sclerosing cholangitis
PTBD	Percutaneous transhepatic biliary drainage
PTC	Percuatneous Transhepatic Cholangiography
PVP	Portal venous phase
RAO	Right Anterior Oblique
RARE	Rapid Acquisition Relaxation Enhancement
RF	Radio frequency
ROI	Region of interest
SSFP	Steady State Free Precession
SSFSE	Steady State Fast Spin Echo
T1WI	T1 weighted image
T2WI	T2 weighted image
TE	Time to Echo
TLC	Tumor-to-liver contrast
US	Ultrasonography
VR	Volume rendering

# CHAPTER I

# Introduction And Aim Of The Work

#### INTRODUCTION

In patients with biliary obstruction, determining the level and the cause of the obstruction is essential because it can be a key factor for the next step in diagnostic or therapeutic intervention. (1\*)

Many imaging modalities are available today for the evaluation of patients with suspected biliary obstruction including Ultrasonography, Computed Tomography and Invasive cholangiography. Magnetic resonance cholangiopancreatography is a relatively new technique, which has gained popularity because of its excellent diagnostic capabilities in the evaluation of biliary obstruction. (2\*)

Multi-detector row CT (MDCT) is a major advance in the field of diagnostic imaging. Cholangiopancreatographic images can be produced using a workstation with advanced postprocessing techniques such as multiplanar reformations (MPR) and minimum intensity projections (MIP). The MPR images using MDCT gives rapid assessment of the pancreaticobiliary ducts along different planes without loosing information about the surrounding structures. The combined use of MPR and MIP techniques significantly improves the images of the pancreatic and bile ducts and their site of confluence compared with those obtained by the axial CT. (3\*)

Magnetic resonance cholangiopancreatography (MRCP) is a unique noninvasive technique for the diagnosis of biliary obstruction. MRCP